Electroproduction of D and B mesons in high-multiplicity ep collisions

Marat Siddikov and Iván Schmidt

Departamento de Física, Universidad Técnica Federico Santa María, y Centro Científico—Tecnológico de Valparaíso, Casilla 110-V, Valparaíso, Chile

(Received 27 March 2021; accepted 28 June 2021; published 30 July 2021)

In this paper, we study the electroproduction of open heavy flavor D and B mesons in the kinematics of future ep colliders, such as the Electron Ion Collider (EIC), the Large Hadron electron Collider (LHeC), and the Future Circular Collider (FCC-he). We study in detail the dependence of the cross sections on multiplicity of coproduced hadrons, in view of its possible sensitivity to contributions from multi-Pomeron contributions, and discuss different observables which might be used for its study. According to our theoretical expectations, in ep collisions the multi-Pomeron contributions are small in the EIC kinematics, although they might be sizable at LHeC and FCC-he. We also provide theoretical predictions for the production cross sections of heavy mesons in the kinematics of all the above-mentioned ep colliders.

DOI: 10.1103/PhysRevD.104.016032

I. INTRODUCTION

Because of the high luminosity of the forthcoming LHC upgrade (HL-LHC) and future electron-proton colliders, many rare processes recently got renewed theoretical interest. One of the directions which might benefit from the outstanding luminosity is the production of different hadrons in high-multiplicity events. The development of a theoretical framework for the study of such events was initiated more than 40 years ago in Refs. [1–6]. However, for a long time, the experimental study of such processes was limited by the insufficient luminosity of existing high-energy experiments (see, however, the discussion in Refs. [7–12] related to HERA). At RHIC and LHC, thanks to the very large luminosity, the multiplicity dependence of hadroproduction processes has been studied in great detail, and various elaborate observables have been measured experimentally, extending our understanding of the mechanisms of these processes. For example, the experimental data revealed that the multiplicity dependence of the light charged hadrons accompanying a heavy hadron is different from the multiplicity dependence of the same light hadrons measured in inclusive production [13–18]. As was suggested in Refs. [19–23], this result might be explained by contributions of higher-twist multi-Pomeron mechanisms. This finding is important, because it gives the possibility to understand better the onset of saturation in high-energy collisions.

It is expected that the future Electron Ion Collider (EIC) [24,25], the Large Hadron electron Collider (LHeC) [26], and the Future Circular Collider (FCC-he) [27–29] also will have very large luminosities, which will make possible a study of physics at the intensity frontier in electroproduction processes. The measurement of the multiplicity dependencies at these new colliders might be used for better understanding of the underlying microscopic mechanisms of different *electroproduction* processes. In what follows, we will focus on the production of heavy flavor D and B mesons, as well as nonprompt J/ψ mesons. These states might be described approximately in the heavy quark mass limit [30,31] and for this reason have been used since the early days of QCD as a probe for testing the predictions of perturbative quantum chromodynamics (QCD) (see, e.g., [32–40] for an overview). The dominant contribution to the inclusive heavy meson production comes from the kinematics with relatively small Q^2, not exceeding a few GeV^2. In this kinematics the typical values of Bjorken x_B are small, $x_B \ll 1$, and the gluon densities significantly exceed the sea quark contributions. In the proton rest frame, the process might be viewed as a scattering of the color dipole, formed from the photon, in the proton gluonic field. The appropriate description of such a process is the color dipole framework (also known as CGC/Sat) [9,41–55]. This approach has been successfully applied to the phenomenological description of both hadron-hadron and lepton-hadron collisions [56–63] and allows a straightforward extension for the description of high-multiplicity events [10,11,39,64–70]. The underlying assumptions of the color dipole approach become invalid for larger values

of $x_B \gtrsim 0.01$. For this reason, in what follows we will consider only the variables which do not get significant contributions from that region. We also will analyze explicitly the role of the multi-Pomeron mechanisms, which are usually omitted as higher-twist effects. Since such contributions have a more pronounced dependence on multiplicity, their presence could be straightforwardly deduced from experimental data on multiplicity dependence.

The paper is structured as follows. In Sec. II, we discuss the framework used for the open heavy meson production evaluation, taking into account the contributions of the single- and double-Pomeron mechanisms, compare the theoretical expectations with experimental data, and make predictions for the kinematics of the future electron-proton colliders. In Sec. III, we suggest the observables which might help to measure the multiplicity dependence and make theoretical predictions for them in the dipole framework. Finally, in Sec. IV, we draw conclusions.

II. PRODUCTION OF OPEN HEAVY FLAVOR MESONS

The cross section of open heavy flavor meson production via the fragmentation mechanism is given by [34,35,39,40,71–73]

$$\frac{d\sigma_{ep\to M+X}}{dx_B dy d\eta d^2p_T} = \sum_i \int_{x_B}^1 \frac{dz}{z^2} D_i\left(\frac{x_B}{z}\right) \frac{d\sigma_{ep\to \bar{Q}_i Q_i+X}}{dx_B dy d\eta^* d^2p_T^*}, \quad (1)$$

where we use standard deep inelastic scattering (DIS) notations Q^2, x_B, and y for the virtuality of intermediate photon, Bjorken variable x_B, and elasticity (fraction of electron energy which passes to the photon in the proton rest frame), respectively; the variable $W^2 \equiv s_{\gamma p} = Q^2(x_B^{-1} - 1) + m_N^2$ stands for the square of the invariant mass of the colliding photon and proton, while η and p_T are the rapidity and the transverse momentum, respectively, of the produced heavy meson. The fragmentation function $D_i(z)$ describes the probability of fragmentation of the parton i into a heavy meson. For D and B meson production, as well as for nonprompt J/ψ production, the corresponding fragmentation functions are known from the literature [34,35,74]. While in Eq. (1) there is a sum over all parton flavors, the dominant contribution to all the mentioned states stems from the heavy c and b quarks. This implies that the cross section $d\sigma_{pp\to \bar{Q}_i Q_i+X}/d\eta d^2p_T$ for heavy quark production might be evaluated in the heavy quark mass limit. It is convenient to separate explicitly the leptonic and hadronic parts of the cross section and rewrite it as [73,75]

$$\frac{d\sigma_{ep\to \bar{Q}_i Q_i+X}}{d\eta d^2p_T} = \frac{\alpha_{\rm em} Q^2}{(s_{ep} - m^2)\pi}\left[(1-y)\frac{d\sigma_L}{d\eta d^2p_T} + \left(1 - y + \frac{y^2}{2}\right)\frac{d\sigma_T}{d\eta d^2p_T}\right], \quad (2)$$

where $d\sigma_L$ and $d\sigma_T$ in the right-hand side of Eq. (2) correspond to the cross sections of heavy quark production by a longitudinally and transversely polarized photon, respectively. In the literature, the results for leptonic processes are frequently discussed in terms of these photon-proton cross sections $d\sigma_{L,T}$, which have simpler structure. In the dipole approach, the cross sections $d\sigma_{L,T}$ are given by

$$\frac{d\sigma_a}{d\eta d^2p_T} = \int_0^1 dz \int \frac{d^2r_1}{4\pi}\int \frac{d^2r_2}{4\pi} e^{i(\boldsymbol{r}_1-\boldsymbol{r}_2)\cdot\boldsymbol{p}_T} \Psi_a^\dagger(r_2,z)\Psi_a(r_1,z)\int d^2\boldsymbol{b} N_M(x_B;\boldsymbol{r}_1,\boldsymbol{r}_2,\boldsymbol{b}), \qquad a = L,T, \quad (3)$$

where η and $\boldsymbol{p}_T$ are the rapidity and transverse momenta, respectively, of the produced heavy meson; $\Psi_a(r,z)$ is the $\bar{Q}Q$ component of the light-cone wave function of the photon; $\boldsymbol{r}_{1,2}$ are the transverse separation between quarks in the amplitude and its conjugate; while z is the light-cone fraction of the photon momentum carried by the quark. For Ψ_a, in the heavy quark mass limit we may use the standard perturbative expressions [76,77]

$$\Psi_T^\dagger(r_2,z,Q^2)\Psi_T(r_1,z,Q^2) = \frac{\alpha_s N_c}{2\pi^2}\{\epsilon_f^2 K_1(\epsilon_f r_1)K_1(\epsilon_f r_2)[e^{i\theta_{12}}z^2 + e^{-i\theta_{12}}(1-z)^2] + m_f^2 K_0(\epsilon_f r_1)K_0(\epsilon_f r_2)\}, \quad (4)$$

$$\Psi_L^\dagger(r_2,z,Q^2)\Psi_L(r_1,z,Q^2) = \frac{\alpha_s N_c}{2\pi^2}\{4Q^2z^2(1-z)^2 K_0(\epsilon_f r_1)K_0(\epsilon_f r_2)\}, \quad (5)$$

where θ_{12} is the azimuthal angle between vectors $\boldsymbol{r}_1$ and $\boldsymbol{r}_1$ and m_f is the mass of the quark of flavor f (in what follows, we use the values $m_c \approx 1.27$ GeV for charm and $m_b \approx 4.2$ GeV for bottom quarks). We also introduced standard shorthand notations

$$\epsilon_f^2 = z(1-z)Q^2 + m_f^2, \quad (6)$$

$$|\Psi^{(f)}(r,z,Q^2)|^2 = |\Psi_T^{(f)}(r,z,Q^2)|^2 + |\Psi_L^{(f)}(r,z,Q^2)|^2. \tag{7}$$

The meson production amplitude N_M depends on the mechanism of the $Q\bar{Q}$ pair formation. As is shown in the Appendix, for the case of production on a single Pomeron (see the left panel in Fig. 1), the amplitude N_M is given by [42,50,78]

$$N_M^{(1)}(x,\vec{\boldsymbol{r}}_1,\vec{\boldsymbol{r}}_2,\vec{\boldsymbol{b}}) = \frac{1}{2}[N(x,\vec{\boldsymbol{r}}_1,\vec{\boldsymbol{b}}) + N(x,\vec{\boldsymbol{r}}_2,\vec{\boldsymbol{b}}) - N(x,\vec{\boldsymbol{r}}_1-\vec{\boldsymbol{r}}_2,\vec{\boldsymbol{b}})], \tag{8}$$

where $N(x,r,b)$ is the amplitude of the color singlet dipole scattering. For numerical estimates of this contribution, we need to fix a parametrization of the amplitude $N(x,r,b)$. In what follows, for the sake of definiteness we will use the CGC parametrization, which was proposed in Refs. [79–82]; more precisely, we will use the impact parameter-dependent fit from Ref. [80]:

$$N(x,\vec{\boldsymbol{r}},\vec{\boldsymbol{b}}) = \sigma_0 \times \begin{cases} N_0\left(\frac{rQ_s(x,b)}{2}\right)^{2\gamma_{\rm eff}(x,r,b)}, & r \le \frac{2}{Q_s(x,b)}, \\ 1-\exp\left(-\mathcal{A}\ln\left(\mathcal{B}rQ_s(x,b)\right)\right), & r > \frac{2}{Q_s(x,b)}, \end{cases} \tag{9}$$

$$\mathcal{A} = -\frac{N_0^2\gamma_s^2}{(1-N_0)^2\ln(1-N_0)}, \qquad \mathcal{B} = \frac{1}{2}(1-N_0)^{-\frac{1-N_0}{N_0\gamma_s}}, \tag{10}$$

$$Q_s(x,\boldsymbol{b}) = \left(\frac{x_0}{x}\right)^{\lambda/2} e^{-\frac{b^2}{4\gamma_s B_{\rm CGC}}}, \qquad \gamma_{\rm eff}(x,r,b) = \gamma_s + \frac{1}{\kappa\lambda Y}\ln\left(\frac{2}{rQ_s(x,b)}\right), \tag{11}$$

$$\gamma_s = 0.6599, \qquad \lambda = 0.2063, \qquad B_{\rm CGC} = 5.5\ {\rm GeV}^{-2}, \qquad x_0 = 1.05\times 10^{-3}, \tag{12}$$

$$Y = \ln(1/x), \tag{13}$$

and for heavy quarks we adjusted the value of argument x as $x = x_B(1+4m_Q^2/Q^2)$ [80].

As we can see from Fig. 2, the single-Pomeron contribution provides a very reasonable description of the available data from HERA. In Figs. 3 and 4, we have shown the theoretical expectations for the cross sections of $D^{\pm}$, $B^{\pm}$, and nonprompt J/ψ meson production, in the kinematics of the future accelerators EIC ($\sqrt{s}_{ep}$ up to 141 GeV), LHeC ($\sqrt{s}_{ep} \approx 1.3$ TeV), and FCC-he ($\sqrt{s}_{ep} \approx 3.5$ TeV) [24–29].

It is also interesting to understand the role of the multi-Pomeron mechanisms in electroproduction. While sometimes it is assumed that all such contributions are taken into account by the universal dipole cross section, in reality the situation is more complicated. The CGC parametrization [63,79–81], used for our numerical estimates, does not take into account such corrections. Another widely used parametrization of the dipole cross section, the so-called b-Sat

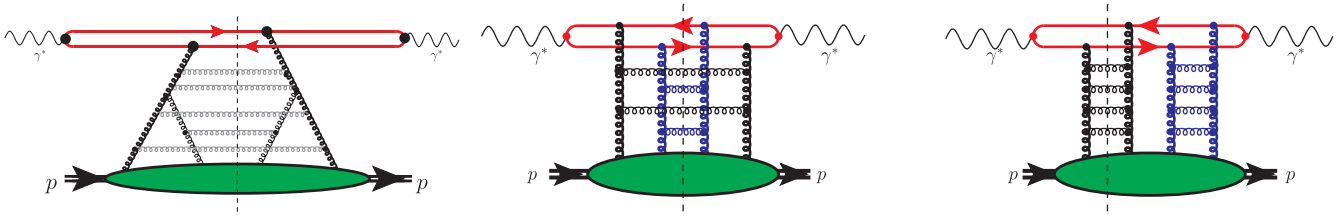

FIG. 1. Left plot: the dominant contribution to electroproduction of heavy quark pairs (single-Pomeron contribution). The dipole amplitude [63,79–81], being the solution of the Balitsky-Kovchegov (BK) equation, effectively includes all possible fanlike contributions shown by the horizontal gray lines (resummation of all possible fanlike topologies is implied). Central and right plots: possible higher-twist contributions due to multi-Pomeron (two-Pomeron) mechanisms. For the sake of legibility, the fanlike structures were simplified down to simple gluon ladders (as in BFKL). The difference in the number of cut Pomerons in the central and right plots will lead to a difference of multiplicity distributions. In all plots, the vertical dashed gray line stands for the unitarity cut, and the blob in the lower part is the hadronic target (proton); the fermionic loop in the upper part of the figure includes a summation over all possible gluons.

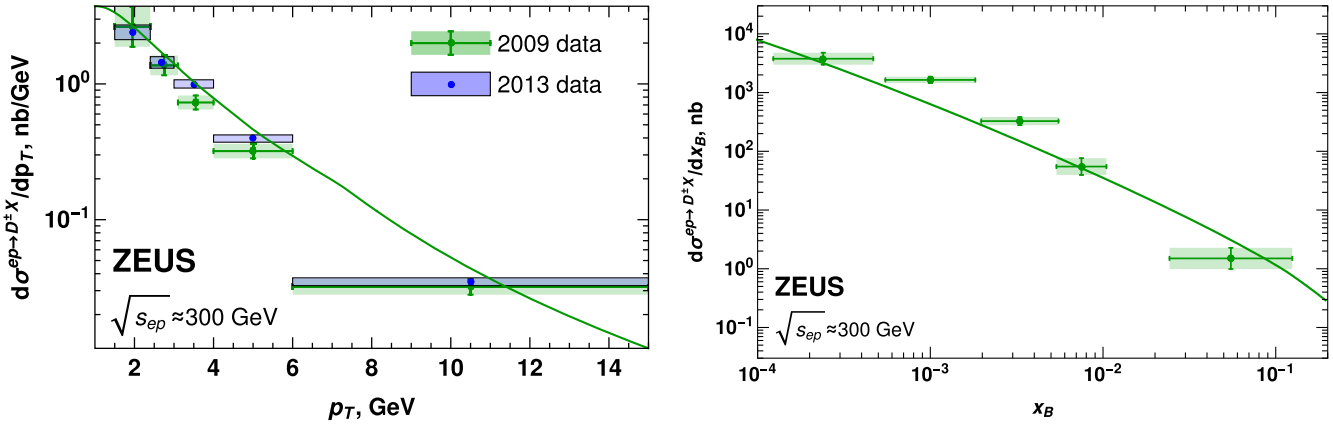

FIG. 2. The p_T and x_B dependence of the D meson production cross section for D^+ mesons in the leading twist (single Pomeron) contribution. The experimental data are from Refs. [83,84]. Additional cuts $5 \lesssim Q^2 \lesssim 1000$ GeV^2, $0.02 \lesssim y \lesssim 0.7$ are imposed both in theoretical curves and in the experimental points, as discussed in Refs. [83,84]. The choice of the lower cutoff $Q^2_{\min} \approx 5$ GeV^2 restricts x_B to the region $x_B \gtrsim Q^2_{\min}/s_{ep} \sim 10^{-4}$. For D^0 mesons, the dependence on the kinematic variables p_T and x_B has a similar shape, although it differs by a numerical factor of 2.

[75,82], takes into account such corrections, making additional simplifying assumptions. For this reason, our goal is to perform a microscopic evaluation using the CGC model. We understand that a systematic evaluation of all such corrections in high-multiplicity events presents a challenging problem, and for this reason we will focus on the contribution of two-Pomeron mechanisms, which are shown in the central and right panels in Fig. 1. Formally, such contributions are expected to be small, because they are of higher twist. However, it is desired to reassess them for electroproduction, because earlier studies [23] revealed that for *hadroproduction* such corrections might be pronounced in the charm sector and in small-p_T kinematics, especially for high-multiplicity events. In what follows, we will refer to the diagrams shown in the central and right panels in Fig. 1 as genuine and interference corrections (in view of the clear interference nature of the latter). For both types of contributions, the corresponding cross section has the familiar structure (3), so these corrections might be rewritten as an additional contribution to the amplitude N_M given by (see derivation in the Appendix)

$$N_M^{(2)}(x,\vec{r}_1,\vec{r}_2,\vec{b}) = N_M^{(\text{genuine})}(x,z,\vec{r}_1,\vec{r}_2,\vec{b}) + N_M^{(\text{int})}(x,z,\vec{r}_1,\vec{r}_2,\vec{b}), \tag{14}$$

where

$$N_M^{(\text{genuine})}(x,z,\vec{r}_1,\vec{r}_2,\vec{b}) \approx \frac{1}{8}\left[N_+^2(x,z,\vec{r}_1,\vec{r}_2,\vec{b})\left(\frac{3N_c^2}{8}\right) + N_-^2(x,\vec{r}_1,\vec{r}_2,\vec{b})\left(\frac{(43N_c^4 - 320N_c^2 + 720)}{72N_c^2}\right) + \frac{(N_c^2-4)}{2}N_+(x,z,\vec{r}_1,\vec{r}_2,\vec{b})N_-(x,\vec{r}_1,\vec{r}_2,\vec{b})\right], \tag{15}$$

$$N_M^{(\text{int})}(x,z,\vec{r}_1,\vec{r}_2,\vec{b}) = -\frac{3}{16}\left[2N_+(x,z,\vec{r}_1,\vec{r}_2)\tilde{N}_+(x,z,\vec{r}_2,\vec{b})\left(\frac{3N_c^2}{8}\right) - N_-(z,\vec{r}_1,\vec{r}_2)\tilde{N}_-(x,\vec{r}_2,\vec{b})\left(\frac{(43N_c^4 - 320N_c^2 + 720)}{72N_c^2}\right) + \frac{(N_c^2-4)}{2}(N_+(z,\vec{r}_1,\vec{r}_2,\vec{b})\tilde{N}_-(x,\vec{r}_2,\vec{b}) + \tilde{N}_+(x,\vec{r}_2,\vec{b})N_-(z,\vec{r}_1,\vec{r}_2,\vec{b}))\right], \tag{16}$$

and we introduced the shorthand notations

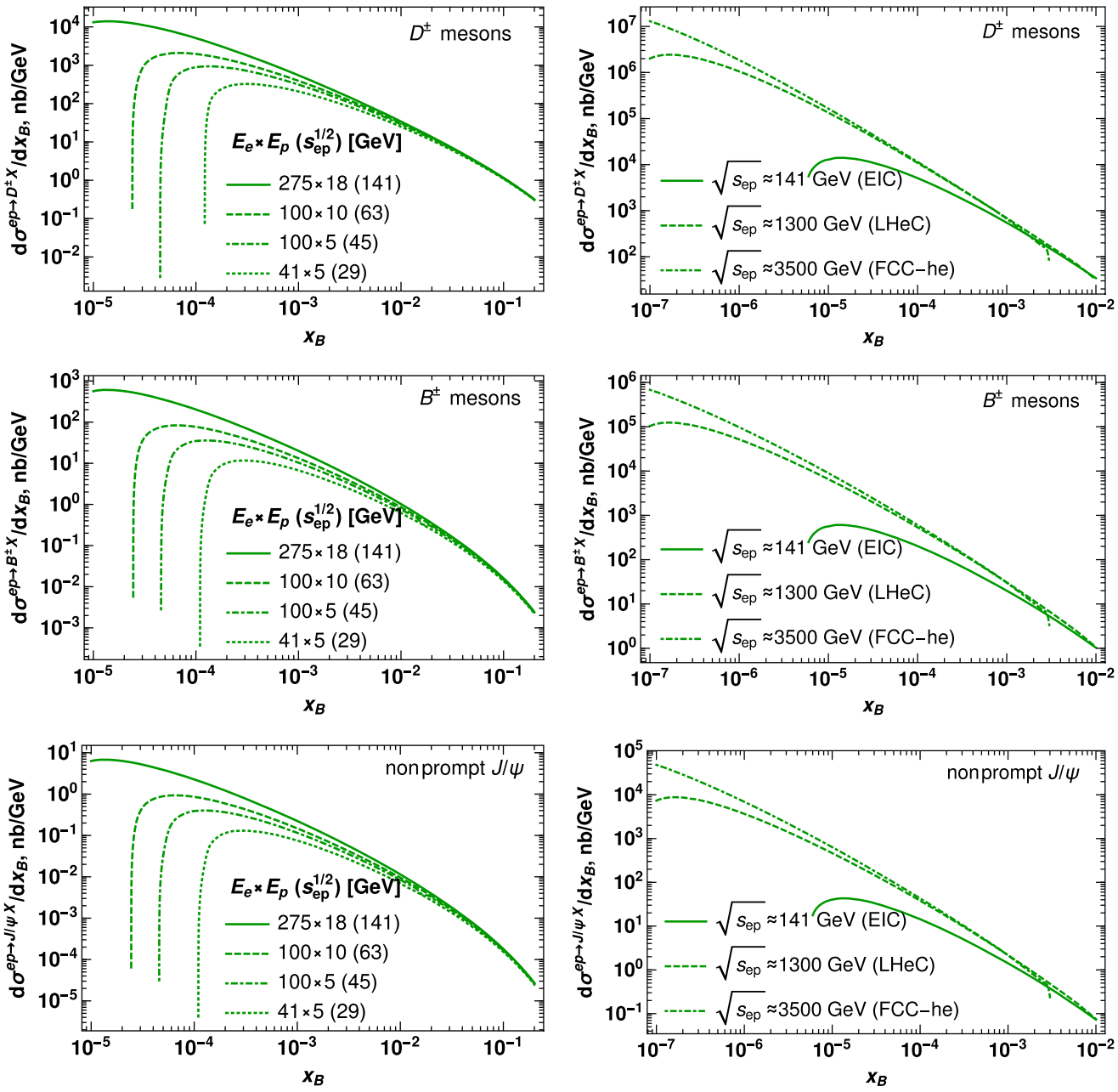

FIG. 3. The x_B dependence of the production cross section for D mesons (upper row), B mesons (central row), and nonprompt J/ψ mesons (lower row). The left column corresponds to different energy sets in the kinematics of the future EIC; the right column corresponds to predictions for LHeC and FCC-he accelerators. For the sake of brevity, we consider only charged D^+ and B^+ mesons; for other D and B mesons, the x_B dependence has a similar shape, although it differs by a numerical factor of 2.

$$N_-(x,\vec{r}_1,\vec{r}_2,\vec{b}) \equiv -\frac{1}{2}[N(x,\vec{r}_2-\vec{r}_1,\vec{b}) - N(x,\vec{r}_1,\vec{b}) - N(x,\vec{r}_2,\vec{b})] = N_M^{(1)}(x,\vec{r}_1,\vec{r}_2,\vec{b}), \tag{17}$$

$$\begin{aligned} N_+(x,z,\vec{r}_1,\vec{r}_2,\vec{b}) \equiv & -\frac{1}{2}[N(x,\vec{r}_2-\vec{r}_1,\vec{b}) + N(x,\vec{r}_1,\vec{b}) + N(x,\vec{r}_2,\vec{b})] \\ & + N(x,\bar{z}\vec{r}_1-\vec{r}_2,\vec{b}) + N(x,\bar{z}\vec{r}_1,\vec{b}) + N(x,-\bar{z}\vec{r}_2+\vec{r}_1,\vec{b}) + N(x,-\bar{z}\vec{r}_2,\vec{b}) - 2N(x,\bar{z}(\vec{r}_1-\vec{r}_2,\vec{b})). \end{aligned} \tag{18}$$

The derivation of these expressions is straightforward and follows the procedures described in Refs. [23,40,50,51]. Both functions $N_{\pm}(z,\vec{r}_1,\vec{r}_2)$ are invariant with respect to the permutation $\boldsymbol{r}_1 \leftrightarrow \boldsymbol{r}_2$. The p_T-integrated cross sections get contributions only from $\vec{r}_1 = \vec{r}_2 = \vec{r}$, so the cross sections $N_{\pm}$ simplify to

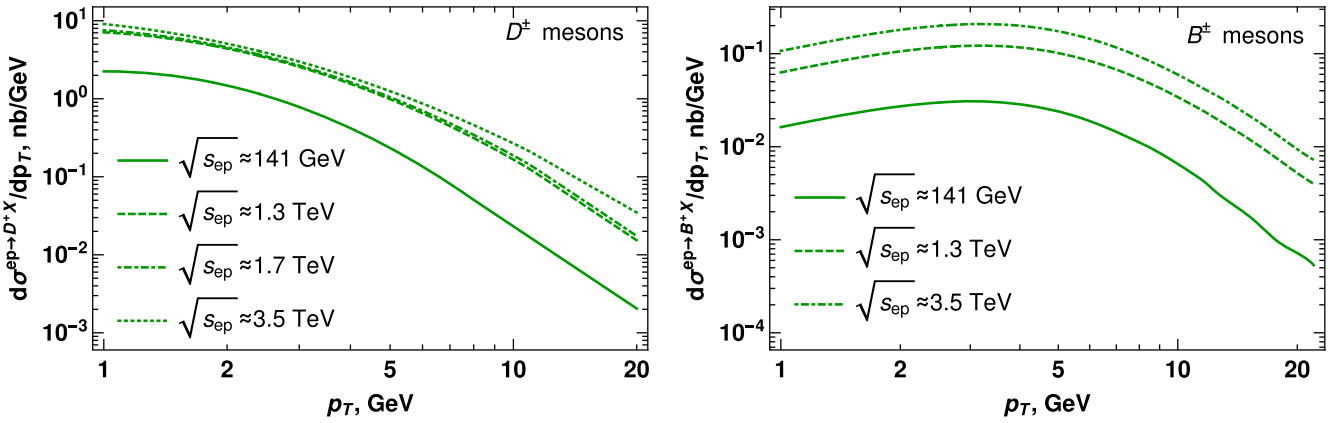

FIG. 4. The p_T dependence of the $D^{\pm}$ and $B^{\pm}$ meson production cross section $d\sigma/dp_T$ in the kinematics of the future accelerators EIC ($\sqrt{s_{ep}} \approx 141$ GeV), LHeC ($\sqrt{s_{ep}} \approx 1.3$–$1.7$ TeV), and FCC-he ($\sqrt{s_{ep}} \approx 3.5$ TeV). The difference between the shapes of the D and B mesons in the small-p_T kinematics stems from the difference of masses of the b and c quarks. For the sake of definiteness, we consider only charged mesons; for other D and B mesons, the p_T dependence has a similar shape, although it differs by a numerical factor of 2.

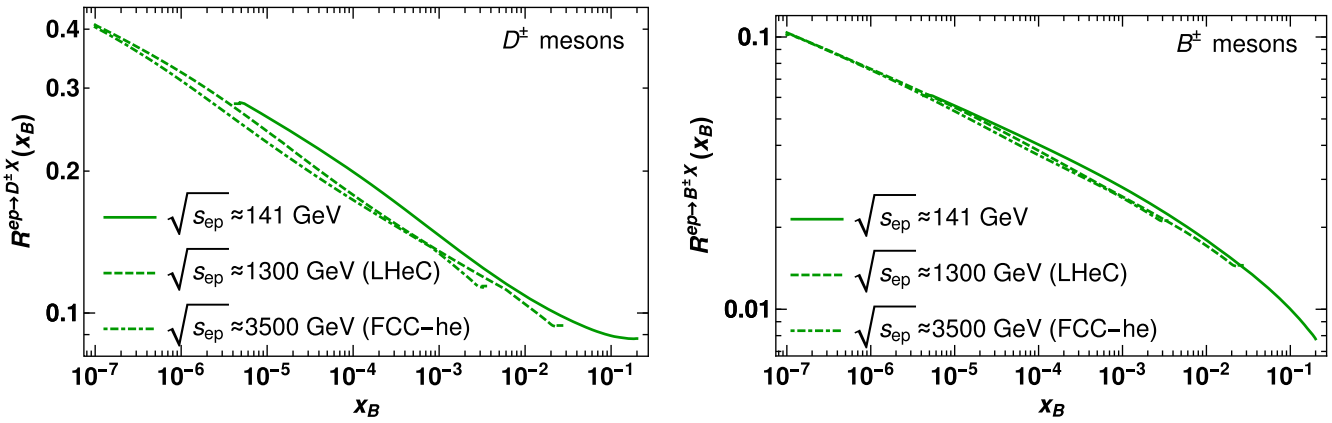

FIG. 5. The ratio of the two-Pomeron and single-Pomeron contributions, defined in Eq. (21), in the kinematics of future accelerators. For the sake of definiteness, we consider D^+ and B^+ mesons; for other D or B mesons as well as for nonprompt J/ψ, the ratio has a very similar shape. The region $x \lesssim 5 \times 10^{-6}$ is kinematically forbidden for EIC energy, and for this reason the solid curve abruptly vanishes there.

$$\tilde{N}_-(x,\vec{\boldsymbol{r}},\vec{\boldsymbol{b}}) \equiv N_-(x,\vec{\boldsymbol{r}},\vec{\boldsymbol{r}},\vec{\boldsymbol{b}}) = N(x,\vec{\boldsymbol{r}},\vec{\boldsymbol{b}}), \tag{19}$$

$$\tilde{N}_+(x,z,\vec{\boldsymbol{r}},\vec{\boldsymbol{b}}) \equiv N_+(x,z,\vec{\boldsymbol{r}},\vec{\boldsymbol{r}},\vec{\boldsymbol{b}}) = 2N(x,\bar{z}\vec{\boldsymbol{r}},\vec{\boldsymbol{b}}) + 2N(x,z\vec{\boldsymbol{r}},\vec{\boldsymbol{b}}) - N(x,\vec{\boldsymbol{r}},\vec{\boldsymbol{b}}). \tag{20}$$

In Fig. 5, we show the ratio of cross sections, where the numerator and denominator were evaluated using the two-Pomeron contribution (14) and the single-Pomeron contribution (8), respectively:

$$R(x_B) = \frac{d\sigma^{(2)}_{ep\to DX}/dx_B}{d\sigma^{(1)}_{ep\to DX}/dx_B}. \tag{21}$$

As we can see from Fig. 5, in the kinematics of EIC, the ratio is quite small. However, the situation is different in the kinematics of the future LHeC and FCC-he colliders, which might probe significantly smaller values of x_B. In that kinematics, the values of the two-Pomeron contributions might reach up to 40% of the total result in the charm sector.

III. MULTIPLICITY DEPENDENCE

The theoretical study of the multiplicity dependence in high-energy collisions was initiated long ago in Refs. [1–6] in the framework of the Regge approach. Relying on very general properties of particle-Reggeon vertices, which are largely independent of the underlying quantum field theory, it was suggested that the enhanced multiplicity of high-energy final states could be considered as one of the manifestations of the multiple Pomeron contributions. Later, it was demonstrated in Refs. [7–12] that all these findings are also valid in the context of QCD and, thus, could be confirmed by experimental evidence. The dependence on multiplicity differs from the dependencies on other kinematic variables which are sometimes used for the extraction of dipole amplitudes, fragmentation functions, or parton distributions from experimental data. This implies that the multiplicity dependence might be used as a litmus test to probe the role of multi-Pomeron contributions.

The probability distribution $P(N_{\rm ch}, \langle N_{\rm ch}\rangle)$ of the high-multiplicity fluctuations inside each Pomeron decreases rapidly as a function of the number of produced charged particles $N_{\rm ch}$, as was found both at ep and pp collisions [85,86]. The theoretical modeling of the essentially nonperturbative probability distribution $P(N_{\rm ch}, \langle N_{\rm ch}\rangle)$ is very challenging. However, in the case of hadroproduction, it is expected [87–91] that resummation of all Pomerons attached to colliding hadrons should yield a multiplicity-dependent factor $\mathcal{P}(n)$, common for the inclusive and semi-inclusive cross sections. In order to exclude this common nonperturbative factor, it is convenient to analyze the multiplicity dependence of the *ratio* of two different processes. For this reason, in pp collisions usually the results are presented for the ratio of cross sections of heavy meson and inclusive processes in a given multiplicity class, self-normalized to one for $n \equiv N_{\rm ch}/\langle N_{\rm ch}\rangle = 1$ for the sake of convenience [13–15,18,92]. Effectively, such a ratio is proportional to a *conditional* probability to measure a hadron provided $N_{\rm ch}$ charged particles are produced in the final state. It was found that in hadroproduction of charm such ratios grow with multiplicity, which clearly indicates pronounced multi-Pomeron contributions. Since the electrons do not participate in strong interactions, the number of possible production mechanisms is significantly reduced compared to the case of hadroproduction. In the *inclusive* electroproduction case, the dominant contribution comes from the light quarks interacting with a proton via exchange of Pomerons. If there are no cuts imposed on the possible values of virtuality Q^2, then there is no formal parameter which would restrict the sizes of the dipoles, and for this reason the dynamics of this process is essentially nonperturbative. We expect that after resummation of all Pomeron diagrams it will be possible to restore the probability distribution $\mathcal{P}(n)$, which appears in hadroproduction. In contrast, in the case of D and B meson electroproduction, the heavy quark mass plays the role of the hard scale, which suppresses the contribution of each additional Pomeron connected to the heavy quark line, and, thus, the multiplicity dependence of this process will be completely different from the inclusive electroproduction. For this reason, the ratio of heavy meson and inclusive electroproduction cross sections does not make much sense as an observable, and new variables are required for the study of multiplicity dependence. Potentially, the contribution of large dipoles might be suppressed in some special kinematics (e.g., at large virtualities Q^2); however, it will be very challenging to measure multiplicity dependences in this kinematics due to significantly smaller statistics. For this reason, below we will consider other variables which might present interest for studies of multiplicity dependence.

The extension of the CGC/Sat framework for description of high-multiplicity events has been discussed in detail in Refs. [10,11,39,64–70,93]. This extension is based on the expectation that in such collisions the dipole amplitude should still satisfy the Balitsky-Kovchegov equation (and, thus, maintain its form), although the saturation scale $Q_s(x,b)$, which controls the onset of the nonlinear dynamics, might be modified. It was shown in Refs. [64–67] that $Q_s(x,b)$ might be related to the observed multiplicity $dN_{\rm ch}/dy$ of soft hadrons as

$$\frac{dN_{\rm ch}}{dy} = c\frac{Q_s^2}{\bar{\alpha}_S(Q_s^2)}, \tag{22}$$

where c is some numerical coefficient. Numerical solution of Eq. (22) allows one to extract Q_s^2 as a function of $dN_{\rm ch}/dy$. For practical applications, it is more convenient to replace the distribution $dN_{\rm ch}/dy$ with the relative enhancement of the multiplicity in a given multiplicity class, $n = N_{\rm ch}/\langle N_{\rm ch}\rangle \approx (dN_{\rm ch}/dy)/\langle dN_{\rm ch}/dy\rangle$. With a reasonable precision, the logarithmic dependence on n due to the running coupling in Eq. (22) might be disregarded, thus reducing Eq. (22) to a very simple form [10,11,64–70]:

$$Q_s^2(x,b;n) = nQ^2(x,b). \tag{23}$$

For multi-Pomeron configurations, we should take into account that multiplicity fluctuations occur independently in each Pomeron, and the observed multiplicity n might be shared in all possible ways between all cut Pomerons in a given rapidity window. However, as was discussed in detail in Refs. [19,20,94], with good precision we may assume

that the observed multiplicity n is shared equally between all Pomerons which participate in the ep process. Using this assumption, as well as certain convolution properties of $P(N_{\rm ch}, \langle N_{\rm ch}\rangle)$, it is possible to show that for the ratio of some electroproduction cross sections the probability distribution $P(N_{\rm ch}, \langle N_{\rm ch}\rangle)$ cancels altogether. Thus, for the evaluation of the cross sections in a given multiplicity class, we may use a simple prescription (23), properly adjusting the parameter n in each Pomeron in order to take into account equal sharing of total multiplicity.

As we can see from Figs. 6 and 7, the theoretical estimates suggest that in high-multiplicity events the role of the multi-Pomeron contributions increases. From comparison of these two figures, we may conclude that the ratio also gradually increases as a function of $\sqrt{s}$, in agreement with theoretical expectations. Numerically, in EIC kinematics this contribution becomes pronounced at $n \gtrsim 5$ for D mesons, although it still remains relatively small for B mesons. This difference in the size of multi-Pomeron terms suggests that we can study experimentally the multiplicity dependence of the ratio of D and B meson cross sections in order to estimate unambiguously the role of the two-Pomeron contribution in D meson production. In order to avoid the effects related to the x_B dependence, we suggest to study the double ratio of cross sections

$$R^{D/B}(x_B, n) = \frac{d\sigma^{D^+}(x_B, n)/d\sigma^{D^+}(x_B, n=1)}{d\sigma^{B^+}(x_B, n)/d\sigma^{B^+}(x_B, 1)}. \quad (24)$$

This ratio equals one in the heavy quark mass limit, although for finite values of n it deviates from this value due to larger contributions of higher-twist corrections for the D meson [numerator of Eq. (24)]. In the left panel in Fig. 8, we show the dependence of the ratio (24) on n. This dependence is pronounced even for the leading single-Pomeron contribution, since the nontrivial structure of the dipole amplitude (9) for the large-size dipoles precludes a complete cancellation of multiplicity dependencies of the D and B meson in the ratio (24). However, the dependence on n becomes significantly stronger when the multi-Pomeron contributions are taken into account. The growth of the ratio as a function of n agrees with the elevated contribution of multi-Pomeron mechanisms in the large-n kinematics. However, we expect that for asymptotically large values of n the ratio should saturate, because the multi-Pomeron contributions will also become important in the denominator.

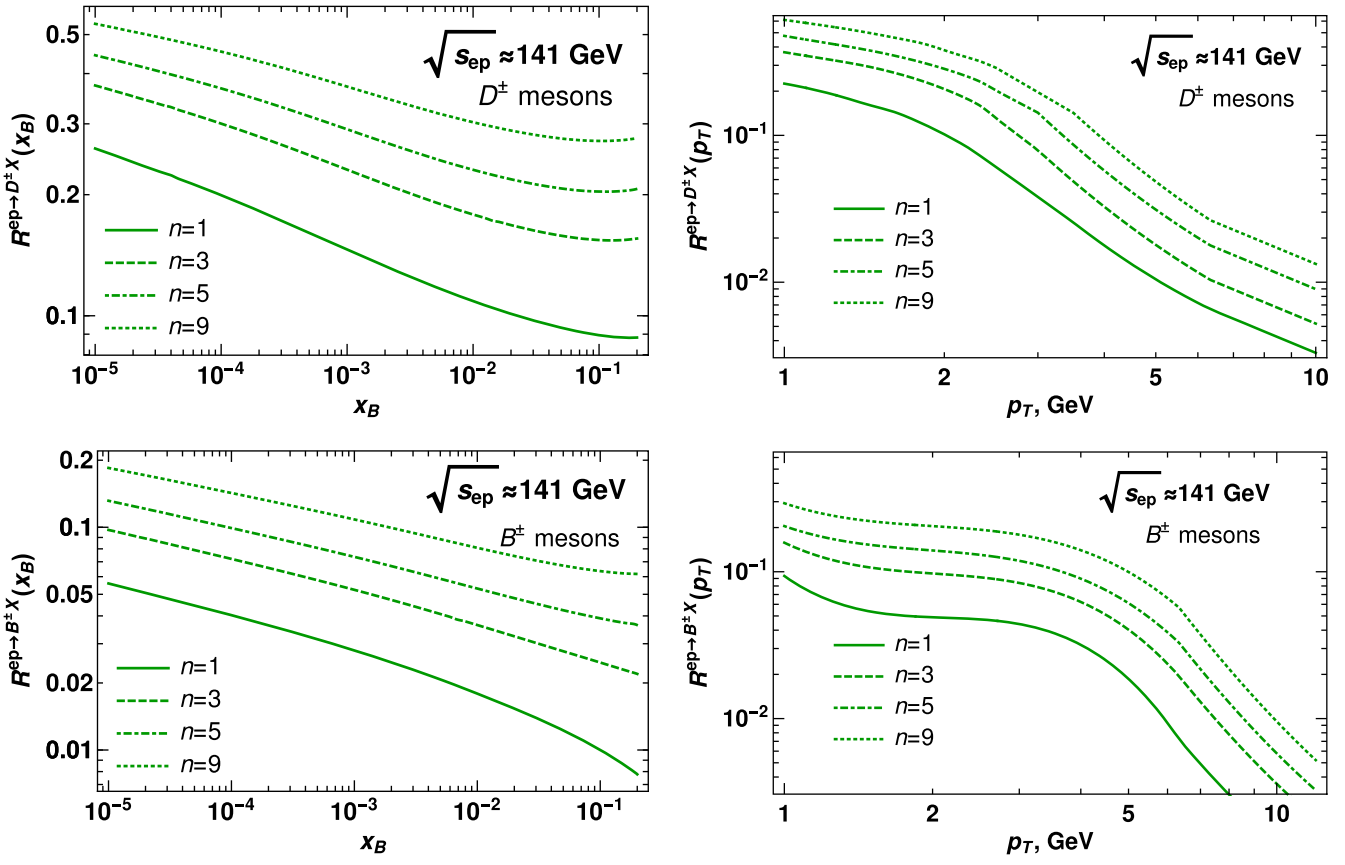

FIG. 6. The ratio (21) of the two-Pomeron to single-Pomeron contributions, as a function of x_B (left diagram) and p_T (right diagram) for electron-proton collision energy $\sqrt{s} = 141$ GeV (EIC kinematics). The upper row corresponds to $D^\pm$ mesons, and the lower row is for $B^\pm$ mesons. The variable $n \equiv N_{\rm ch}/\langle N_{\rm ch}\rangle$ is the relative enhancement of multiplicity.

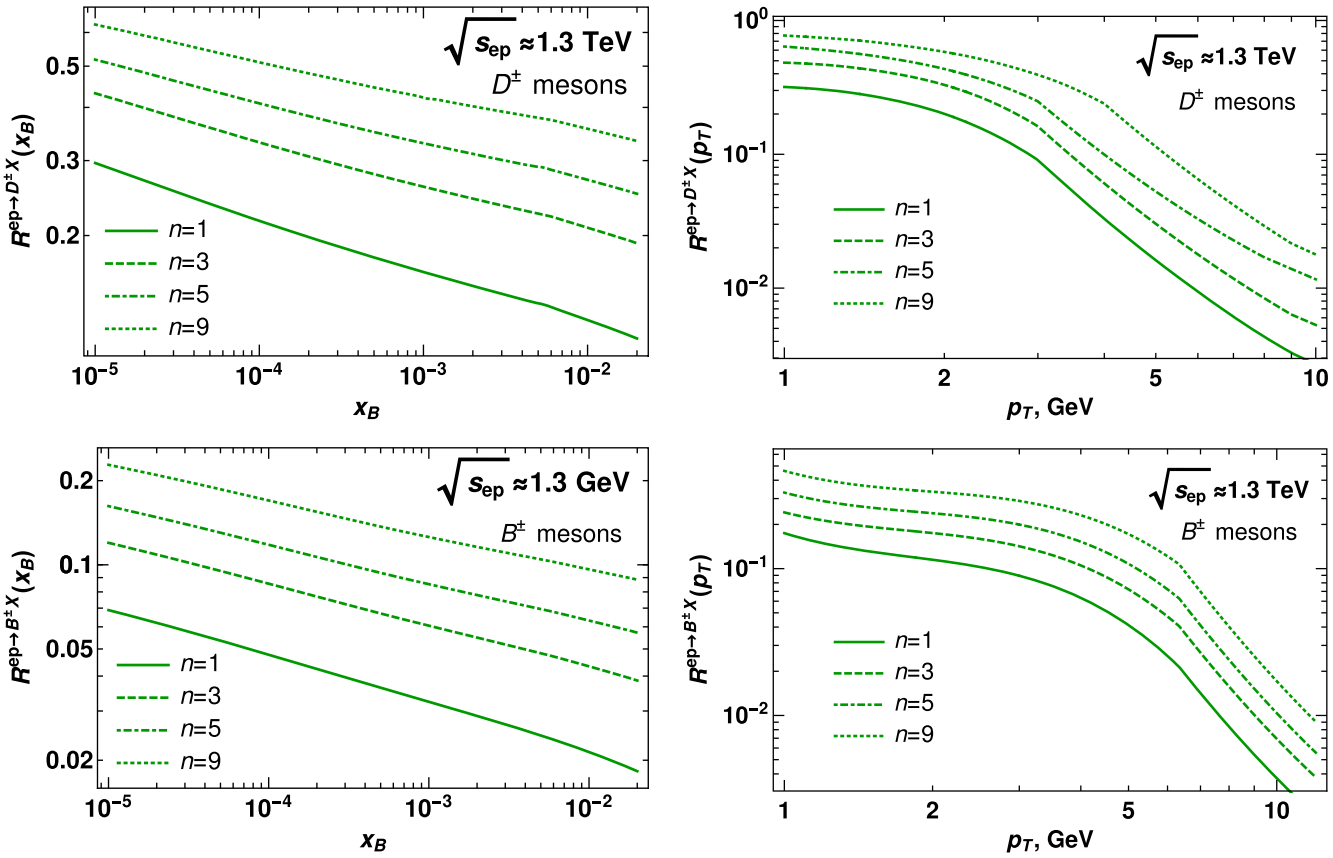

FIG. 7. The ratio (21) of the two-Pomeron to single-Pomeron contributions, as a function of x_B (left diagram) and p_T (right diagram) for electron-proton collision energy $\sqrt{s} = 1.3$ TeV (LHeC kinematics). The upper row corresponds to $D^{\pm}$ mesons, and the lower row is for $B^{\pm}$ mesons. The variable $n \equiv N_{\rm ch}/\langle N_{\rm ch}\rangle$ is the relative enhancement of multiplicity.

In the right panel in Fig. 8, we show a similar self-normalized double ratio (24), in which we replaced B mesons with nonprompt D mesons. Since the latter mechanism is dominated by b quark decays, we can see that qualitatively the ratio has a similar dependence on n. Comparison of the left and right panels in Fig. 8 clearly illustrates that the enhancement of the ratio (24) is not related to differences of the D and B meson fragmentation functions. We expect that nonprompt charmonia should demonstrate a similar behavior.

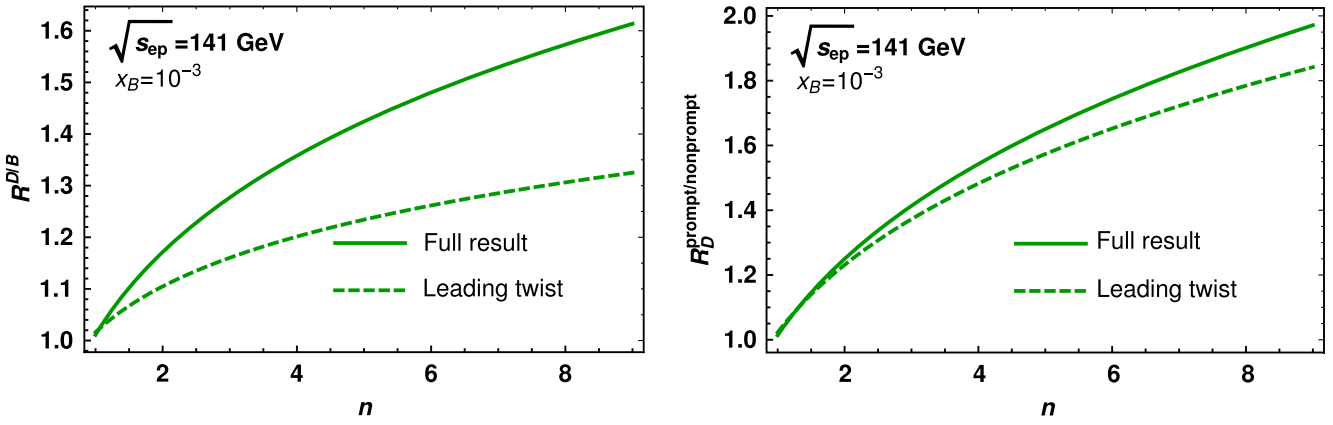

FIG. 8. Left plot: the self-normalized ratio of D^+ and B^+ meson cross sections, as defined in Eq. (24). Right plot: self-normalized ratio of the prompt and nonprompt D meson cross sections, defined similar to Eq. (24), but with B mesons replaced by nonprompt D meson cross section in the denominator. The dashed curve, with label "leading twist," stands for the leading twist (single-Pomeron) contribution.

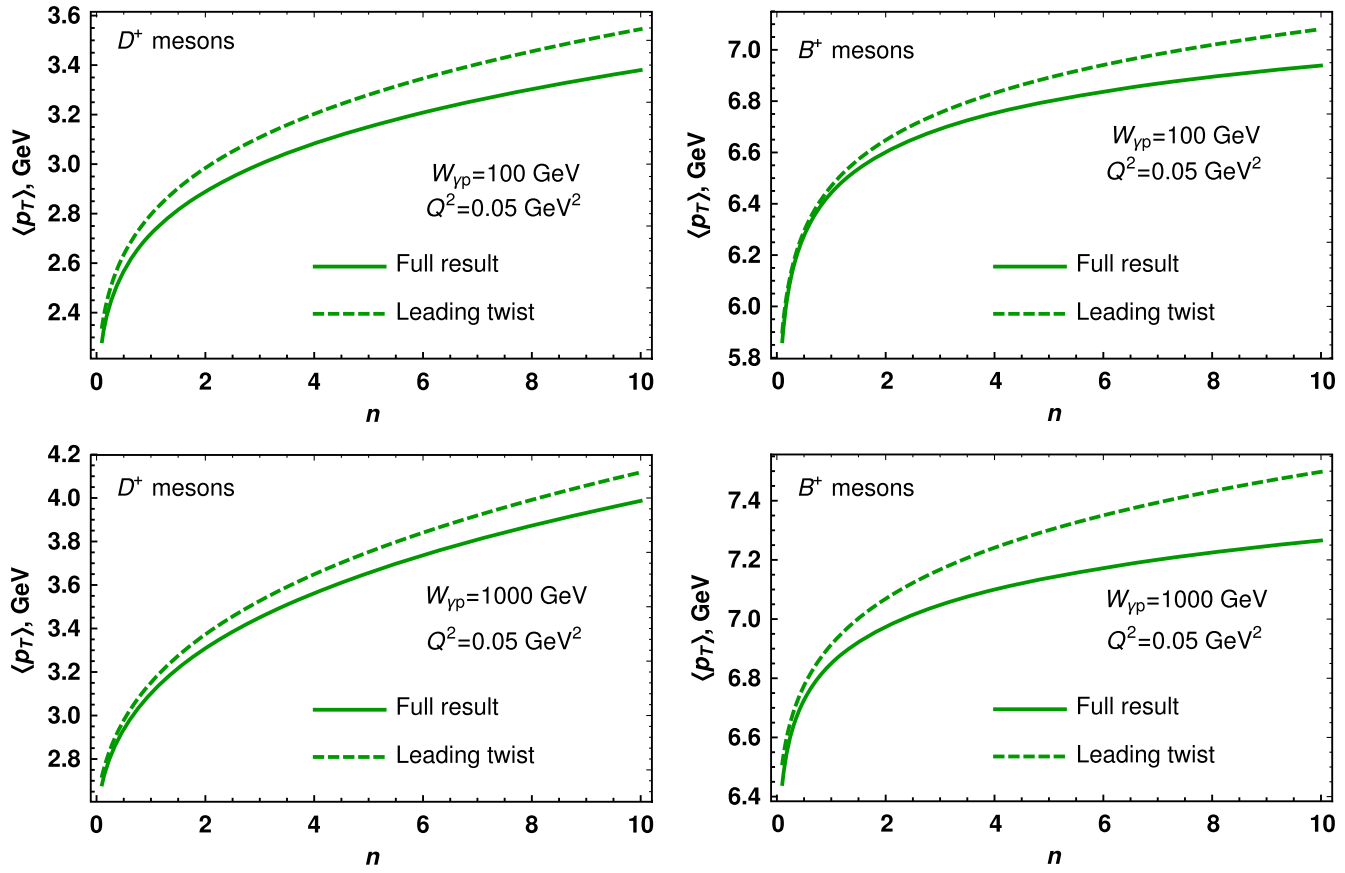

FIG. 9. The multiplicity dependence of average $\langle p_T \rangle$ of produced D mesons (left column) and B mesons (right column). The upper row corresponds to the invariant photon energy $W_{\gamma p} \approx 100$ GeV (EIC kinematics), whereas the lower row corresponds to higher energy $W_{\gamma p} \approx 1000$ GeV, achievable at both LHeC and FCC-he. The dashed curve with label "leading twist" in all plots stands for the leading twist (single-Pomeron) contribution.

Another observable which might be measured experimentally is the dependence of the average momentum $\langle p_T \rangle$ of heavy mesons on the multiplicity n. This observable has been extensively studied in the context of pp collisions. In Fig. 9, we show the dependence of $\langle p_T \rangle$ on n, for electroproduction of both D and B mesons. Since multi-Pomeron contributions are suppressed at large momenta p_T, we can see that their inclusion decreases the average $\langle p_T \rangle$, compared to what is expected from a single Pomeron. Although the expected effect is not very large, we believe that it might be seen in experimental data, since $\langle p_T \rangle$ might be measured with very good precision.

In summary, we believe that the multiplicity dependence might reveal information about the contribution of the multi-Pomeron mechanisms. However, in EIC kinematics, we do not expect drastic enhancement of the multiplicity dependence, as was observed in pp collisions. This happens because, in general, multi-Pomeron contributions are small at EIC energies. The situation might be different in the kinematics of future accelerators like LHeC and FCC-he, where the role of the multi-Pomeron contributions is more pronounced. In our analysis, we took into account only the first multi-Pomeron correction, namely, the production on two Pomerons. We could see that its relative contribution is small in EIC kinematics, in agreement with general expectations based on twist counting, and for this reason we do not consider the corrections of even higher order. However, at very small values of x_B (significantly smaller than 10^{-7}), we approach the deeply saturated regime, where the expectations based on twist expansion are not reliable, and, thus, the inclusion of all higher twist might be required.

The mechanism of multiplicity generation suggested in this section introduces dependence on the multiplicity of soft produced particles and is quite different from other approaches, such as the percolation approach [95] or the modification of the slope of the elastic amplitude [96], suggested earlier in the context of pp studies. We expect that the experimental confirmation of the predicted multiplicity dependence could help to understand better the mechanisms of multiplicity enhancement in high-energy collisions.

IV. CONCLUSIONS

In this paper, we analyzed the mechanisms of open heavy flavor meson electroproduction. Motivated by earlier findings in pp collisions, we also analyzed the relative contribution of the first subleading multi-Pomeron correction. We found that for electroproduction this correction is relatively small for EIC kinematics, although it grows with energy and becomes relevant for charm production at LHeC and FCC-he, especially in the small-p_T kinematics. This correction is less important for B mesons and nonprompt charmonia production and does not exceed 10% even at LHeC and FCC-he. The dependence of the correction on p_T agrees with general expectations based on large-p_T and heavy quark mass limit. Our evaluation is largely parameter-free and describes very well the data from HERA, as well as provides plausible predictions for EIC, LHeC, and FCC-he.

We also analyzed the multiplicity dependence, which might be studied experimentally in detail at future EIC, LHeC, and FCC-he, due to its outstanding luminosity. The high-multiplicity events present special interest for theoretical studies, because they allow one to get better understanding of the production mechanisms at high gluon densities. Since the probability of rare high-multiplicity events is exponentially suppressed, for the analysis of their dynamics it is important to study the properly designed variables. We analyzed in detail the dependence on multiplicity for the average momentum of heavy meson $\langle p_T \rangle$ and the double ratio defined in Eq. (24). The first variable is easier to measure, although it is less sensitive to higher-twist effects, due to the smallness of subleading contributions. The double ratio (24) is more interesting, because its deviations from unity allow one to quantify directly the size of the higher-twist corrections, including multi-Pomeron contributions. Because of the smallness of multi-Pomeron contributions, we do not expect a significant relative enhancement of the cross sections at large multiplicity in EIC kinematics and only mild enhancement in the kinematics of LHeC and FCC-he. This expectation differs significantly from what was found experimentally in pp collisions at LHC [13]. We expect that the experimental confirmation of these findings could help to understand better the mechanisms of multiplicity generation in high-energy collisions.

ACKNOWLEDGMENTS

We thank our colleagues at UTFSM university for encouraging discussions. This research was partially supported by Proyecto ANID PIA/APOYO AFB180002 (Chile) and Fondecyt (Chile) Grant No. 1180232. Also, we thank Yuri Ivanov for technical support of the USM HPC cluster where a part of evaluations has been done.

APPENDIX: EVALUATION OF THE DIPOLE AMPLITUDES

In this Appendix, we explain briefly the evaluation of the diagrams shown in Fig. 1, which eventually yields the expressions (8), (15), and (16). The discussion of the framework which allows one to rewrite the cross section of a high-energy process in terms of the color singlet dipole amplitudes might be found in Refs. [43–51]. Though technically the general rules formulated by different authors might slightly differ at some intermediate steps, finally they all are known to give the equivalent expressions.

In the Iancu-Mueller approach [97] (see also [11]), the interaction of the dipole with the target is described by the S-matrix element

$$S(\boldsymbol{x},\boldsymbol{y}) = \frac{1}{N_c}\langle V^\dagger(\boldsymbol{x})V(\boldsymbol{y})\rangle, \tag{A1}$$

where $y = \ln(1/x)$ is the rapidity of the dipole and $V^\dagger(\boldsymbol{x})$ and $V(\boldsymbol{y})$ in Eq. (A1) are Wilson lines describing the scattering of the quark and antiquark with transverse coordinates $\boldsymbol{x}$, $\boldsymbol{y}$ in the color field of a hadron:

$$V(\boldsymbol{x}_\perp) = P\exp\left(ig\int dx^- A_a^+(x^-,\boldsymbol{x}_\perp)t^a\right), \tag{A2}$$

and A_μ^a is the gluonic field. The dipole amplitude $N(x,\boldsymbol{r})$, which is probed in DIS, and its impact-parameter-dependent extension $N(x,\boldsymbol{r},\boldsymbol{b})$ might be related to $S(y,\boldsymbol{x},\boldsymbol{y})$ as

$$N(x,\boldsymbol{r},\boldsymbol{b}) = 1 - S(y,\boldsymbol{x},\boldsymbol{y}), \tag{A3}$$

$$N(x,\boldsymbol{r}) = \int d^2b N(x,\boldsymbol{r},\boldsymbol{b}), \tag{A4}$$

$$\boldsymbol{r} = \boldsymbol{x} - \boldsymbol{y}, \tag{A5}$$

$$\boldsymbol{b} = z\boldsymbol{x} + \bar{z}\boldsymbol{y}, \tag{A6}$$

where $z,\bar{z} \equiv 1 - z$ are the light-cone fractions of the dipole carried by the quark and antiquark.

In the heavy quark mass limit, the interaction of the virtual $\bar{Q}Q$ dipole with the gluonic field might be described perturbatively, since the strong coupling $\alpha_s(m_Q)$ becomes small. In this limit, we may see that the interaction of $\bar{Q}$ and Q reduces just to a simple factor $\pm it^a\gamma_a(\boldsymbol{x}_\perp)$, where t^a is the standard color group generator in fundamental representation, $\boldsymbol{x}_\perp$ is the transverse coordinate of the quark or antiquark, and the function $\gamma_a(\boldsymbol{x}_\perp) \sim g\int dx^- A_a^+(x^-,\boldsymbol{x}_\perp)$ characterizes the distribution of gluons in the transverse plane. This result coincides with an earlier formulation in Refs. [50,51], so for this reason from now on we will follow

the notations and procedure described in the latter papers. However, we emphasize that the heavy quark limit does not affect the self-interaction of gluons, as well as their interaction with light quarks, so the evolution of the dipole amplitude $N(x,\boldsymbol{r})$ is still described by the nonlinear Balitsky-Kovchegov equation rather than linearized BFKL. As could be seen from Eq. (A3), for heavy quarks the function γ_a might be related to a dipole scattering amplitude $N(x,\boldsymbol{r})$ as

$$N(x,\boldsymbol{r}) = \frac{1}{N_c^2-1}\int d^2b|\gamma_a(x,\boldsymbol{b}-z\boldsymbol{r}) - \gamma_a(x,\boldsymbol{b}+\bar{z}\boldsymbol{r})|^2, \tag{A7}$$

where $\boldsymbol{r}$ is the transverse size of the dipole, z is the light-cone fraction of the dipole momentum carried by the heavy quark Q, and the factor $(N_c^2-1)^{-1}$ comes from the averaging over color indices of t-channel gluons. The impact parameter dipole amplitude $N(x,\boldsymbol{r},\boldsymbol{b})$ might be obtained from Eq. (A7) just omitting the integral over the impact parameter $\int d^2\boldsymbol{b}$. Equation (A7) might be rewritten in the form

$$\frac{1}{N_c^2-1}\int d^2\boldsymbol{b}\gamma_a(x,\boldsymbol{b})\gamma_a(x,\boldsymbol{b}+\boldsymbol{r}) = \frac{1}{2}N(x,\boldsymbol{r}) + \underbrace{\frac{1}{N_c^2-1}\int d^2b|\gamma_a(x,\boldsymbol{b})|^2}_{=\text{const}}. \tag{A8}$$

The last (constant) term in the right-hand side in Eq. (A8) is related to the infrared behavior of the theory, and for the observables which we consider in this paper it cancels exactly. With the help of Eq. (A8), it is possible to express the production cross sections of various processes as linear combinations of the dipole amplitudes $N(x,\boldsymbol{r})$ with different arguments.

For the electroproduction of heavy flavors, we should take into account the diagrams shown in Fig. 1. The evaluations of the leading twist contribution (leftmost diagram) is straightforward and yields for the square of the amplitude

$$\begin{aligned}|\mathcal{A}_{\gamma^* p\to Q(\boldsymbol{p}_T)\bar{Q}X}|^2 \sim \int dz_1dz_2d^2\boldsymbol{r}_1d^2\boldsymbol{r}_2\int d^2\boldsymbol{b}_1d^2\boldsymbol{b}_2 e^{-i\boldsymbol{p}_T\cdot(\boldsymbol{b}_{12}-z(\boldsymbol{r}_1-\boldsymbol{r}_2))}\\ \times\langle\Psi^\dagger_{\bar{Q}Q}(r_2,z_2)\Psi_M(r_2,z_2)\rangle^*\langle\Psi^\dagger_{\bar{Q}Q}(r_1,z_1)\Psi_M(r_1,z_1)\rangle\\ \times(\gamma_a(\boldsymbol{b}_1+\bar{z}_2\boldsymbol{r}_2)-\gamma_a(\boldsymbol{b}_1-z_2\boldsymbol{r}_2))^*(\gamma_a(\boldsymbol{b}_2+\bar{z}_1\boldsymbol{r}_1)-\gamma_a(\boldsymbol{b}_2-z_1\boldsymbol{r}_1))|_{\boldsymbol{b}_2=\boldsymbol{b}_1+\bar{z}\boldsymbol{r}_1-\bar{z}\boldsymbol{r}_2},\end{aligned} \tag{A9}$$

where $(z_i,\boldsymbol{r}_i)$ stand for the fraction of the dipole momentum carried by the quark and the size of the dipole, $\boldsymbol{b}_i$ is the impact parameter of the dipole, and the subscript index i takes the values $i=1,2$ to distinguish variables in the amplitude and its conjugate. In the arguments of γ, the quark and antiquark transverse coordinates are given by $\boldsymbol{b}_i-z_i\boldsymbol{r}_i$ and $\boldsymbol{b}_i+\bar{z}_i\boldsymbol{r}_i$, respectively. The variable $\boldsymbol{b}_{12}\equiv\boldsymbol{b}_1-\boldsymbol{b}_2$. The factor $\sim e^{-i\boldsymbol{p}_T\cdot(\boldsymbol{b}_{21}-\cdots)}$ in the first line in Eq. (A9) stems from the projection of the produced quark Q onto the eigenstates with definite momentum $\boldsymbol{p}_T$, in both the amplitude and its conjugate. The integration over the kinematics of produced antiquark $\bar{Q}$ leads to equality of transverse coordinates of $\bar{Q}$ in the amplitude and conjugate and yields a relation between impact parameters $\boldsymbol{b}_2=\boldsymbol{b}_1+\bar{z}\boldsymbol{r}_1-\bar{z}\boldsymbol{r}_2$. After straightforward algebraic simplifications with the help of identity (A8), we may get the result (8) known from the literature [42,78]. For the p_T-integrated cross section, we may notice that only configurations with $\boldsymbol{r}_1=\boldsymbol{r}_2$ contribute, and, thus, Eq. (8) simplifies as

$$N_M^{(1)}(x,\vec{\boldsymbol{r}}_1,\vec{\boldsymbol{r}}_1) = N(x,\vec{\boldsymbol{r}}_1). \tag{A10}$$

For the two-Pomeron contribution given in the central and right panels in Fig. 1, the evaluation is very similar to that of the single-Pomeron contribution. In evaluation of the "genuine" contribution shown in the central panel, it is important to take into account that at high energies the dominant contribution comes from the configuration in which the t-channel gluons in the amplitude Reggeize independently (i.e., form two disconnected gluon ladders, split by the unitarity cut). Indeed, as was demonstrated in Ref. [98], all possible multi-Reggeized configurations with arbitrary connections between gluon ladders have a smaller intercept than a pair of isolated Pomerons and for this reason are suppressed at high energies. After interaction with a pair of Pomerons, the $Q\bar{Q}$ dipole might be in either color singlet or color octet states, and its amplitude is given by

$$\mathcal{A}_{ab}(z,\boldsymbol{b},\boldsymbol{r}) = \left[\left(\frac{\delta_{ab}}{6}+\frac{d_{abc}}{2}t_c\right)[\gamma_a(x,\boldsymbol{b}-z\boldsymbol{r})-\gamma_a(x,\boldsymbol{b}+\bar{z}\boldsymbol{r})]+\frac{if_{abc}}{2}t_c[\gamma_b(x,\boldsymbol{b}-z\boldsymbol{r})+\gamma_b(x,\boldsymbol{b}+\bar{z}\boldsymbol{r})]\right]\Psi_{\bar{Q}Q}(\boldsymbol{r},z), \tag{A11}$$

whereas the cross section of the process

$$\begin{aligned} d\sigma^{(\mathrm{genuine})} &\sim |\mathcal{A}^{(\mathrm{genuine})}_{\gamma^* p\to Q(\boldsymbol{p}_T)\bar{Q}X}|^2 \\ &\sim \int dz_1 dz_2 d^2\boldsymbol{r}_1 d^2\boldsymbol{r}_2 \int d^2\boldsymbol{b}_1 d^2\boldsymbol{b}_2 e^{-i\boldsymbol{p}_T\cdot(\boldsymbol{b}_{12}-z(\boldsymbol{r}_1-\boldsymbol{r}_2))}\langle\Psi^\dagger_{\bar{Q}Q}(r_2,z_2)\Psi_M(r_2,z_2)\rangle^*\langle\Psi^\dagger_{\bar{Q}Q}(r_1,z_1)\Psi_M(r_1,z_1)\rangle \\ &\quad\times \mathrm{tr}_c[\mathcal{A}^*_{ab}(z,\boldsymbol{b}_2,\boldsymbol{r}_2)\mathcal{A}^*_{ab}(z,\boldsymbol{b}_1,\boldsymbol{r}_1)]_{\boldsymbol{b}_2=\boldsymbol{b}_1+\bar{z}\boldsymbol{r}_1-\bar{z}\boldsymbol{r}_2}. \end{aligned} \tag{A12}$$

After convolution of the color indices and some straightforward algebraic simplifications with the help of Eq. (A8), it is possible to demonstrate that we obtain the result (15). In a similar fashion, we may reproduce the result (16) for the interference correction.

[1] V. A. Abramovsky, V. N. Gribov, and O. V. Kancheli, Yad. Fiz. **18**, 595 (1973), https://sciencejournals.ru/journal/yadfiz/.
[2] A. Capella and A. Kaidalov, Nucl. Phys. **B111**, 477 (1976).
[3] L. Bertocchi and D. Treleani, J. Phys. G **3**, 147 (1977).
[4] Y. M. Shabelski, Sov. J. Nucl. Phys. **26**, 573 (1977).
[5] N. N. Nikolaev and W. Schafer, Phys. Rev. D **74**, 074021 (2006).
[6] A. B. Kaidalov and K. A. Ter-Martirosian, Phys. Lett. **117B**, 247 (1982).
[7] J. Bartels and M. G. Ryskin, Z. Phys. C **76**, 241 (1997).
[8] J. Bartels, M. Salvadore, and G. P. Vacca, Eur. Phys. J. C **42**, 53 (2005).
[9] Y. V. Kovchegov, Phys. Rev. D **60**, 034008 (1999).
[10] Y. V. Kovchegov, Nucl. Phys. **A692**, 557 (2001).
[11] Y. V. Kovchegov and E. Levin, Cambridge Monogr. Part. Phys., Nucl. Phys., Cosmol. **33**, 1 (2012).
[12] T. Sjostrand and P. Z. Skands, J. High Energy Phys. 03 (2004) 053.
[13] J. Adam *et al.* (ALICE Collaboration), J. High Energy Phys. 09 (2015) 148.
[14] B. Trzeciak (STAR Collaboration), J. Phys. Conf. Ser. **668**, 012093 (2016).
[15] R. Ma (STAR Collaboration), Nucl. Part. Phys. Proc. **276–278**, 261 (2016).
[16] D. Thakur (ALICE Collaboration), arXiv:1811.01535.
[17] A. Khatun (ALICE Collaboration), Springer Proc. Phys. **261**, 599 (2021).
[18] B. Abelev *et al.* (ALICE Collaboration), Phys. Lett. B **712**, 165 (2012).
[19] M. Siddikov, E. Levin, and I. Schmidt, Eur. Phys. J. C **80**, 560 (2020).
[20] E. Levin and M. Siddikov, Eur. Phys. J. C **79**, 376 (2019).
[21] M. Siddikov and I. Schmidt, Phys. Rev. D **102**, 076020 (2020).
[22] M. Siddikov and I. Schmidt, Phys. Rev. D **104**, 016023 (2021).
[23] I. Schmidt and M. Siddikov, Phys. Rev. D **101**, 094020 (2020).
[24] A. Accardi *et al.*, Eur. Phys. J. A **52**, 268 (2016).
[25] R. Abdul Khalek, A. Accardi, J. Adam, D. Adamiak, W. Akers, M. Albaladejo, A. Al-bataineh, M. G. Alexeev, F. Ameli, P. Antonioli *et al.*, arXiv:2103.05419.
[26] J. L. Abelleira Fernandez *et al.* (LHeC Study Group), J. Phys. G **39**, 075001 (2012).
[27] M. Mangano, 3/2017; https://doi.org/10.23731/CYRM-2017-003, arXiv:1710.06353, ISBN: 9789290834533 (Print), 9789290834540 (eBook).
[28] P. Agostini *et al.* (LHeC and FCC-he Study Group), arXiv:2007.14491.
[29] A. Abada *et al.* (FCC Collaboration), Eur. Phys. J. C **79**, 474 (2019); Y. V. Kovchegov, Phys. Rev. D **60**, 034008 (1999).
[30] J. G. Korner and G. Thompson, Phys. Lett. B **264**, 185 (1991).
[31] M. Neubert, Phys. Rep. **245**, 259 (1994).
[32] G. T. Bodwin, E. Braaten, and G. P. Lepage, Phys. Rev. D **51**, 1125 (1995); **55**, 5853(E) (1997).
[33] F. Maltoni, M. L. Mangano, and A. Petrelli, Nucl. Phys. **B519**, 361 (1998).
[34] J. Binnewies, B. A. Kniehl, and G. Kramer, Phys. Rev. D **58**, 034016 (1998).
[35] B. A. Kniehl and G. Kramer, Phys. Rev. D **60**, 014006 (1999).
[36] N. Brambilla, E. Mereghetti, and A. Vairo, Phys. Rev. D **79**, 074002 (2009); **83**, 079904(E) (2011).
[37] Y. Feng, J. P. Lansberg, and J. X. Wang, Eur. Phys. J. C **75**, 313 (2015).
[38] N. Brambilla *et al.*, Eur. Phys. J. C **71**, 1534 (2011).
[39] Y. Q. Ma, P. Tribedy, R. Venugopalan, and K. Watanabe, Phys. Rev. D **98**, 074025 (2018).

[40] V. P. Goncalves, B. Kopeliovich, J. Nemchik, R. Pasechnik, and I. Potashnikova, Phys. Rev. D **96**, 014010 (2017).
[41] A. H. Mueller, Nucl. Phys. **B335**, 115 (1990).
[42] N. N. Nikolaev and B. G. Zakharov, Z. Phys. C **49**, 607 (1991).
[43] L. V. Gribov, E. M. Levin, and M. G. Ryskin, Phys. Rep. **100**, 1 (1983).
[44] L. D. McLerran and R. Venugopalan, Phys. Rev. D **49**, 2233 (1994).
[45] L. D. McLerran and R. Venugopalan, Phys. Rev. D **49**, 3352 (1994).
[46] L. D. McLerran and R. Venugopalan, Phys. Rev. D **50**, 2225 (1994).
[47] A. H. Mueller and J. Qiu, Nucl. Phys. **B268**, 427 (1986).
[48] L. McLerran and R. Venugopalan, Phys. Rev. D **49**, 3352 (1994); Phys. Rev. D **50**, 2225 (1994); Phys. Rev. D **59**, 094002 (1999).
[49] K. J. Golec-Biernat and M. Wusthoff, Phys. Rev. D **60**, 114023 (1999).
[50] B. Z. Kopeliovich and A. V. Tarasov, Nucl. Phys. **A710**, 180 (2002).
[51] B. Kopeliovich, A. Tarasov, and J. Hufner, Nucl. Phys. **A696**, 669 (2001).
[52] Y. V. Kovchegov and H. Weigert, Nucl. Phys. **A784**, 188 (2007).
[53] I. Balitsky and G. A. Chirilli, Phys. Rev. D **77**, 014019 (2008).
[54] I. Balitsky, Phys. Lett. B **518**, 235 (2001).
[55] F. Cougoulic and Y. V. Kovchegov, Phys. Rev. D **100**, 114020 (2019).
[56] C. A. Aidala *et al.*, arXiv:2002.12333.
[57] Y. Q. Ma and R. Venugopalan, Phys. Rev. Lett. **113**, 192301 (2014).
[58] F. Gelis, E. Iancu, J. Jalilian-Marian, and R. Venugopalan, Annu. Rev. Nucl. Part. Sci. **60**, 463 (2010).
[59] J. L. Albacete, N. Armesto, R. Baier, G. G. Barnafoldi, J. Barrette, S. De, W. T. Deng, A. Dumitru, K. Dusling, and K. J. Eskola *et al.*, Int. J. Mod. Phys. E **22**, 1330007 (2013).
[60] J. L. Albacete and C. Marquet, Phys. Lett. B **687**, 174 (2010).
[61] J. L. Albacete, A. Dumitru, H. Fujii, and Y. Nara, Nucl. Phys. **A897**, 1 (2013).
[62] T. Lappi and H. Mäntysaari, Phys. Rev. D **88**, 114020 (2013).
[63] G. Watt and H. Kowalski, Phys. Rev. D **78**, 014016 (2008).
[64] D. Kharzeev and E. Levin, Phys. Lett. B **523**, 79 (2001).
[65] D. Kharzeev, E. Levin, and M. Nardi, Phys. Rev. C, arXiv: hep-ph/0111315.
[66] D. Kharzeev, E. Levin, and M. Nardi, J. Phys. G **35**, 054001 (2008).
[67] A. Dumitru, D. E. Kharzeev, E. M. Levin, and Y. Nara, Phys. Rev. C **85**, 044920 (2012).
[68] D. Kharzeev and M. Nardi, Phys. Lett. B **507**, 121 (2001).
[69] E. Levin and A. H. Rezaeian, Phys. Rev. D **82**, 014022 (2010).
[70] T. Lappi, Eur. Phys. J. C **71**, 1699 (2011).
[71] N. N. Nikolaev, G. Piller, and B. G. Zakharov, Z. Phys. A **354**, 99 (1996).
[72] N. N. Nikolaev, G. Piller, and B. G. Zakharov, J. Exp. Theor. Phys. **81**, 851 (1995), http://www.jetp.ac.ru/cgi-bin/e/index/e/81/5/p851?a=list.
[73] P. A. Zyla *et al.* (Particle Data Group), Prog. Theor. Exp. Phys. (**2020**), 083C01.
[74] T. Kneesch, B. A. Kniehl, G. Kramer, and I. Schienbein, Nucl. Phys. **B799**, 34 (2008).
[75] A. H. Rezaeian, M. Siddikov, M. Van de Klundert, and R. Venugopalan, Phys. Rev. D **87**, 034002 (2013).
[76] H. G. Dosch, T. Gousset, G. Kulzinger, and H. J. Pirner, Phys. Rev. D **55**, 2602 (1997).
[77] J. D. Bjorken, J. B. Kogut, and D. E. Soper, Phys. Rev. D **3**, 1382 (1971).
[78] V. P. Goncalves and M. V. T. Machado, Phys. Rev. D **71**, 014025 (2005).
[79] E. Iancu, K. Itakura, and S. Munier, Phys. Lett. B **590**, 199 (2004).
[80] A. H. Rezaeian and I. Schmidt, Phys. Rev. D **88**, 074016 (2013).
[81] H. Kowalski, L. Motyka, and G. Watt, Phys. Rev. D **74**, 074016 (2006).
[82] H. Kowalski and D. Teaney, Phys. Rev. D **68**, 114005 (2003).
[83] S. Chekanov *et al.* (ZEUS Collaboration), Eur. Phys. J. C **63**, 171 (2009).
[84] I. Abt *et al.* (ZEUS Collaboration), J. High Energy Phys. 05 (2013) 023.
[85] B. Abelev *et al.* (ALICE Collaboration), Phys. Lett. B **712**, 165 (2012).
[86] S. Chekanov *et al.* (ZEUS Collaboration), J. High Energy Phys. 06 (2008) 061.
[87] Y. V. Kovchegov, E. Levin, and L. D. McLerran, Phys. Rev. C **63**, 024903 (2001).
[88] D. Kharzeev, E. Levin, and M. Nardi, Nucl. Phys. **A747**, 609 (2005).
[89] A. Capella and E. G. Ferreiro, Eur. Phys. J. C **72**, 1936 (2012).
[90] A. Dumitru and Y. Nara, Phys. Rev. C **85**, 034907 (2012).
[91] A. Capella and E. G. Ferreiro, arXiv:1301.3339.
[92] D. Thakur (ALICE Collaboration), Springer Proc. Phys. **234**, 217 (2019).
[93] A. Kovner and V. V. Skokov, Phys. Rev. D **98**, 014004 (2018).
[94] E. Levin, Phys. Rev. D **49**, 4469 (1994).
[95] E. G. Ferreiro and C. Pajares, Phys. Rev. C **86**, 034903 (2012).
[96] B. Z. Kopeliovich, H. J. Pirner, I. K. Potashnikova, K. Reygers, and I. Schmidt, Phys. Rev. D **88**, 116002 (2013).
[97] E. Iancu and A. H. Mueller, Nucl. Phys. **A730**, 460 (2004).
[98] G. P. Korchemsky, J. Kotanski, and A. N. Manashov, Phys. Rev. Lett. **88**, 122002 (2002).